

Relationship between solar wind, D_{st} , and plasmasphere mass density on one-hour time scales

Victoir Veibell*

R.S. Weigel†

June 5, 2015

Abstract

This paper looks at how various magnetosphere conditions behave around the onset of geomagnetic storms. It confirms results from previous papers that a sudden drop in D_{st} correlates with a spike in equatorial mass density, while adding a level of depth and specification to the applicability of their results. It compares data at 1-hour averages to data at 1-day averages, and briefly to data at 27-day averages to examine if the trend holds at varying time scales and finds that it does, so long as the data is pre-processed to linearly remove a large time scale $F_{10.7}$ dependence. By then looking at an hourly average of variables from 24 hours before storm onset to 48 hours after, short timescale trends can be discerned.

1 Introduction

Takahashi et al. [2006], show how trends in storm dependence on mass/density only appear in longer timescales. Looking at K_p vs mass (amu) in the range of 6 to 7 R_E , a trend shows up in the 1.5 day averages that doesn't appear in the 3 hour averages.

Denton et al. [2006] show how D_{st} affects the distribution of plasma density along different magnetic latitudes, and specifically along the same field lines as looked at in later papers (6-8 R_E). Though this shows that the trends for density may differ between field lines, it's mentioned mostly as a point for future research as the data used in this paper is already adjusted for one field line, as described by Takahashi et al. [2010].

Yao et al. [2008] looks at the differences in how D_{st} correlates with number density for different ions in different regions (ring current and plasma sheet), but still finds a general correlation during each of the four storms selected.

Takahashi et al. [2010] state that spikes in the Disturbance Storm Time (D_{st}) index coincide with significant changes in ρ_{eq} at an L-shell of 6.8 R_E . For five storms over a 20 day period two had ρ_{eq} spikes after the D_{st} drop, two had ρ_{eq} spikes before the drop,

and one showed little change in ρ_{eq} . They then show an epoch analysis where ρ_{eq} is seen to spike the day of a D_{st} drop, using a daily average of 30 minute ρ_{eq} and one hour D_{st} measurements.

2 Data Preparation

Starting from the data provided by Denton [2007] for ρ_{eq} and $F_{10.7}$ from 1980-1991, and Kondrashov et al. [2014] for all other variables from 1972-2013, the data were prepared to get all variables on the same consecutive time-grid. Since the latter was pre-adjusted to have data on a consecutive one-hour grid, the former variables were adjusted to be compatible. First, since the data covers multiple Geostationary Operational Environmental Satellites (GOES), one in particular (GOES 7) was selected to avoid overlapping data points.

Second, the various forms of "bad data" were converted from their respective set value to NaNs (e.g. 9999 becomes NaN). It was then condensed in range to match the time range from Kondrashov et al. [2014] down to the same start and end hours, and then interpolated from the GOES 15-minute grid to the one-hour grid by taking the median of all valid non-NaN data points within half an hour to either side of each hour. When no valid points existed in that hour period, a NaN was kept for the sake of the uniform time grid.

*vveibell@gmu.edu

†rweigel@gmu.edu

The only other point to note in this section: For finding storm times, all NaNs were linearly interpolated out of the data in order to aid in finding storms that may have had their onset point missing. Though this may skew the onset time slightly, it's thought to be less skewed than trying to determine start and end times with the NaNs in place. This interpolation was only used for determining storm times, and not for any analysis.

3 Results

Figure 1 shows values of solar wind averages and mass density used in this study. We will briefly compare our results to other published results to verify our methods and handling of data.

3.1 D_{st} Events

Two storm indicators are looked at in this study. The first is looking for a drop in DST below the threshold of $-50nT$ specified in Takahashi et al. [2010], dubbed the "onset", and then considering the timeframe a storm until D_{st} passes back above the $-50nT$ threshold. This method finds 669 such periods between May 1983 and August 1991 with an average duration of 9 hours and a median duration of 3 hours. A subset of longer duration storms will be looked at later. Figure 1 shows the average values of B_Z , V_{SW} , D_{st} , $F_{10.7}$, and Mass Density for a period of 24 hours before and 48 hours after a storm onset, as well as a plot of mass density with the found storm times highlighted.

This figure shows a definite spike in the Z component of the magnetic field, as well as the defined drop in DST , but no obvious change in mass density at an hourly timescale. This points to an issue with only looking at long-timescale trends between density and D_{st} , and allows for the possibility that other factors are influencing the long term correlation since there's no obvious connection on a short timescale. One possibility is that, as suggested in Takahashi et al. [2010], $F_{10.7}$ plays a significant role in driving long term density values which biases the long term correlation of density and D_{st} .

3.2 Mass Density Events

Figure 3 shows this same algorithm, but looking for a rise in mass density over a value of $40g/cm^3$. This results in 130 storms with a mean duration of 32 hours and a median duration of 17 hours, marked in red on the left figure.

This shows that when using all data for mass den-

sity derived storms, almost no significant changes can be seen around storm onset.

4 More specific storms

It's hypothesized that progressively picking more specific storm criteria will allow for the possibility of more significant results, at the expense of more bias in the selection process and potentially less overall usefulness of the results. That said, the predictability of extreme storms is of definite interest, so an attempt has been made to find some reproducible method of prediction. Looking at storms that last longer than 12 hours and storms with an onset threshold greater than $70g/cm^3$ results in the left and right sides of Figure 4 respectively.

Neither of these seem to indicate anything too significant, so looking at D_{st} storms instead to look for something that causes a significant change in Mass Density results in Figure 5. This shows that by either looking only at D_{st} storms that last longer than an hour (left) or at storms where the onset condition is $D_{st} < -80nT$, a spike in mass density is seen, but also a definite lack of data availability to the point where that spike may be coming from less than five of the total 143 storms.

Unfortunately there are no storms in this time frame that are longer than 12 hours with D_{st} minima lower than $-80nT$ that have existing mass density data around onset, so an analysis of this particular relationship can't be made.

4.1 Change in ρ_{eq}

If instead of looking for storms based on a threshold of ρ_{eq} , we instead look for a certain amount of change in ρ_{eq} as the basis for storm onset, we get Figure 6.

Both raw change and percent change were done in case of bias towards high or low ρ_{eq} periods, respectively. This shows a distinct lack of correlation in either case to a change in D_{st} . The percent change in ρ_{eq} does, however, seem to be preconditioned by changes in B_z and $F_{10.7}$.

5 $F_{10.7}$ dependence

In an effort to analyze the dependence of ρ_{eq} on $F_{10.7}$, a few tests were performed. Takahashi et al. [2010] mention a strong correlation between the two. The long term correlation could be a bias for D_{st} 's effects, so a linear model was created, recreating mass density purely from $F_{10.7}$ in the form of $\rho_{eq}(t) = A * F_{10.7}(t)$. This re-created ρ_{eq} shows around a 45%

correlation with the actual ρ_{eq} , suggesting a strong influence, while doing the same procedure with DST shows only a 20-25% correlation.

Taking this re-created data set and subtracting it from the original should remove the $F_{10.7}$ dependence from the data, and allow for a less biased analysis of the relationship between D_{st} and ρ_{eq} . Figure 7 shows the stack plot for the reduced $F_{10.7}$, where a more distinct peak after storm onset can be seen. It also shows what that removed trend looks like, of the form $\rho_{eq} - \rho_{eq, F_{10.7}}$.

Similarly, looking at the 1 day averaged data with and without the $F_{10.7}$ dependence, Figure 8 shows that the results of Takahashi et al. [2010] hold only once the dependence has been removed. The 27 day trend couldn't be determined as not enough valid data existed to test it.

References

- K. Takahashi, R. E. Denton, and H. J. Singer. Solar cycle variation of geosynchronous plasma mass density derived from the frequency of standing Alfvén waves. *Journal of Geophysical Research (Space Physics)*, 115:A07207, July 2010. doi:[10.1029/2009JA015243](https://doi.org/10.1029/2009JA015243).
- K. Takahashi, R. E. Denton, R. R. Anderson, and W. J. Hughes. Mass density inferred from toroidal wave frequencies and its comparison to electron density. *Journal of Geophysical Research (Space Physics)*, 111:A01201, January 2006. doi:[10.1029/2005JA011286](https://doi.org/10.1029/2005JA011286).
- B. Lavraud, M. F. Thomsen, J. E. Borovsky, M. H. Denton, and T. I. Pulkkinen. Magnetosphere preconditioning under northward IMF: Evidence from the study of coronal mass ejection and corotating interaction region geoeffectiveness. *Journal of Geophysical Research (Space Physics)*, 111:A09208, September 2006. doi:[10.1029/2005JA011566](https://doi.org/10.1029/2005JA011566).
- B. T. Tsurutani and W. D. Gonzalez. The Interplanetary causes of magnetic storms: A review. *Washington DC American Geophysical Union Geophysical Monograph Series*, 98:77–89, 1997. doi:[10.1029/GM098p0077](https://doi.org/10.1029/GM098p0077).
- R. E. Denton, K. Takahashi, I. A. Galkin, P. A. Nsumei, X. Huang, B. W. Reinisch, R. R. Anderson, M. K. Sleeper, and W. J. Hughes. Distribution of density along magnetospheric field lines. *Journal of Geophysical Research (Space Physics)*, 111:A04213, April 2006. doi:[10.1029/2005JA011414](https://doi.org/10.1029/2005JA011414).
- Y. Yao, K. Seki, Y. Miyoshi, J. P. McFadden, E. J. Lund, and C. W. Carlson. Effect of solar wind variation on low-energy O⁺ populations in the magnetosphere during geomagnetic storms: FAST observations. *Journal of Geophysical Research (Space Physics)*, 113, 2008. doi:[10.1029/2007JA012681](https://doi.org/10.1029/2007JA012681).
- R. Denton. Database of Input Parameters for Tsyganenko Magnetic Field Modles, 2007. URL <http://www.dartmouth.edu/~rdenton/magpar/index.html>. Retrieved 2013-10-28.
- D. Kondrashov, R. Denton, Y. Y. Shprits, and H. J. Singer. Reconstruction of gaps in the past history of solar wind parameters. *Geophysical Research Letters*, 41:2702–2707, April 2014. doi:[10.1002/2014GL059741](https://doi.org/10.1002/2014GL059741).

6 Figures

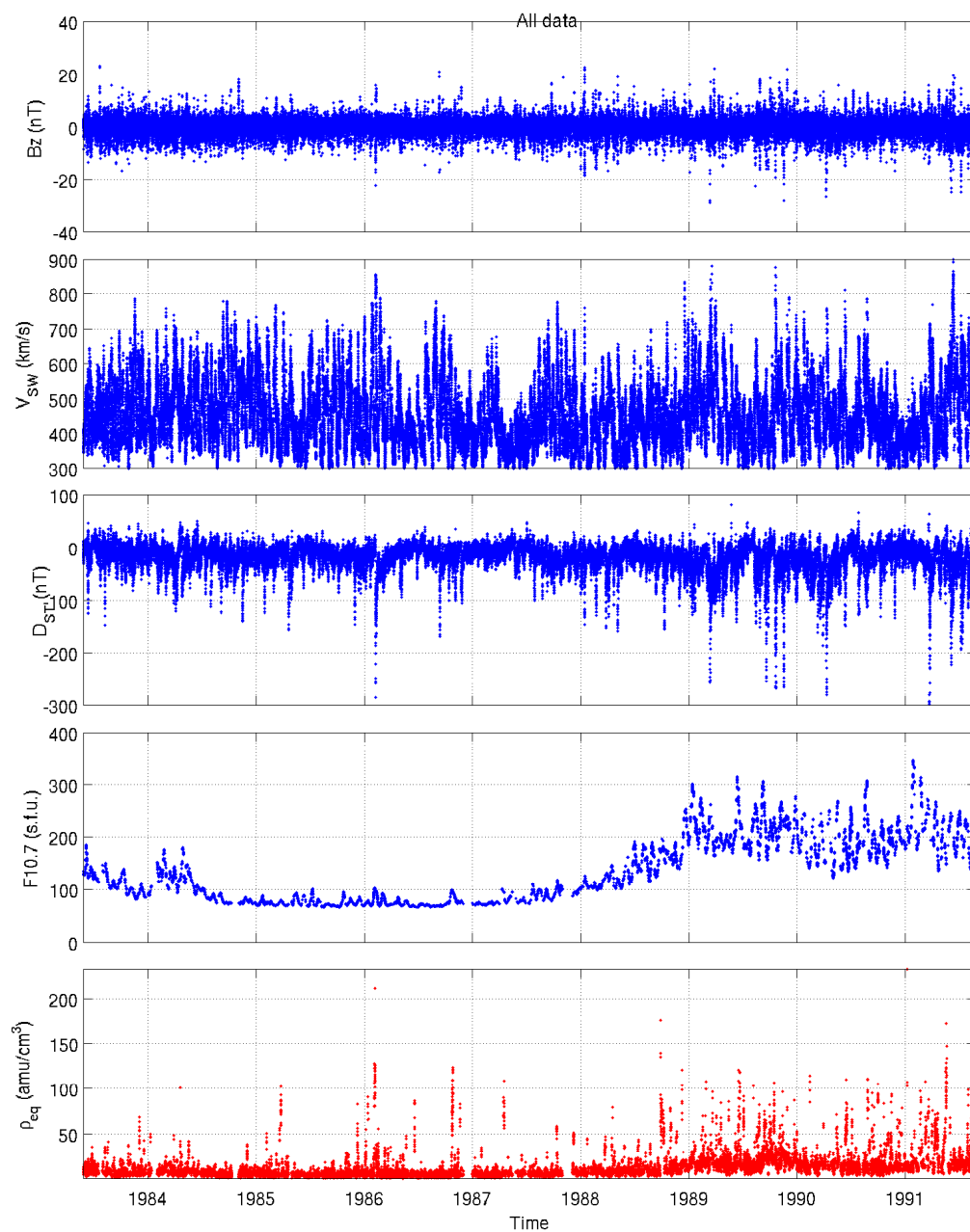


Figure 1: Overview of data used in this study. The top four panels are from [Kondrashov et al. \[2014\]](#) and the bottom panel is based on [Denton \[2007\]](#) after interpolation and averaging described in the text.

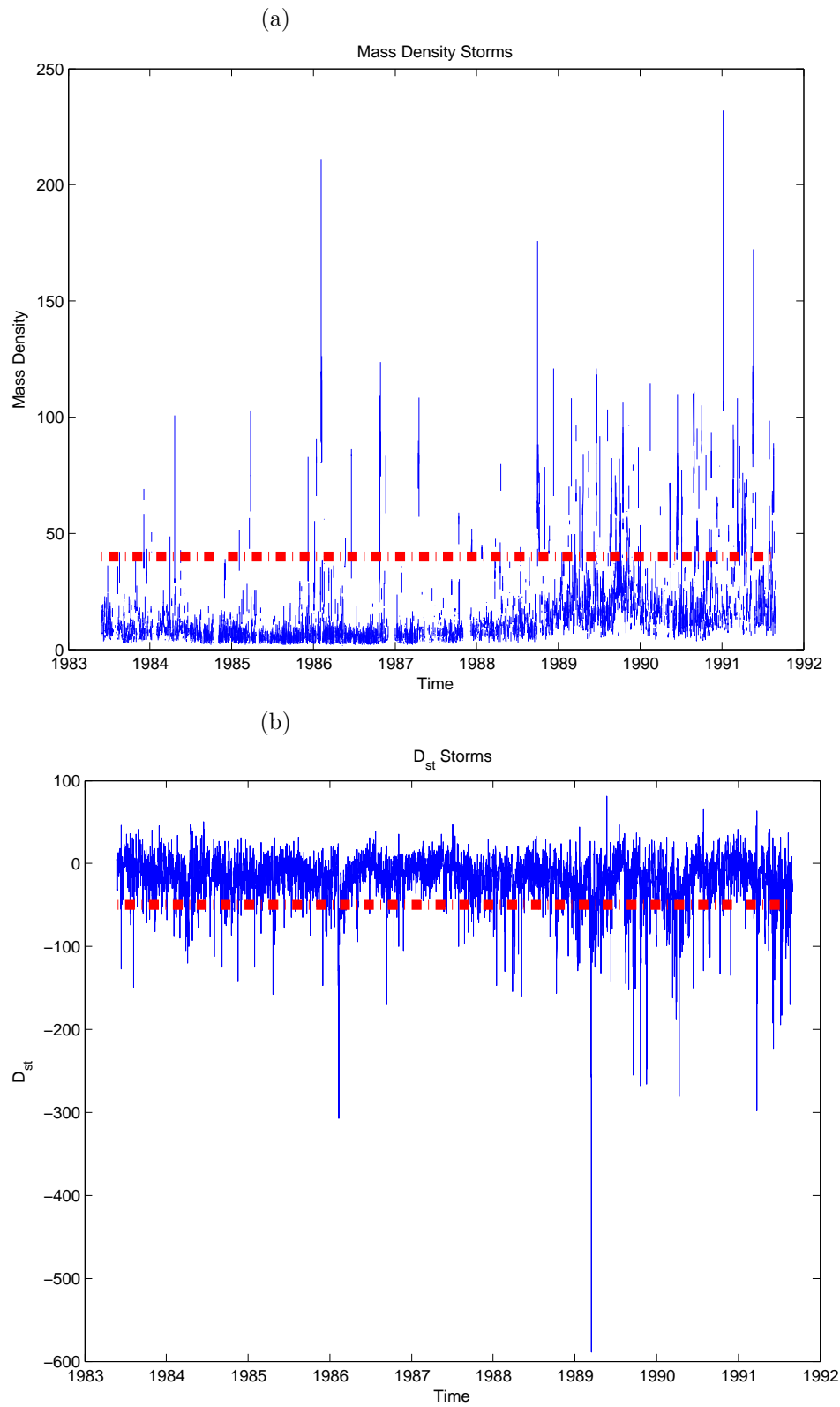


Figure 2: Averages around time of (a) 669 ρ_{eq} and (b) 130 D_{st} events along with thresholds used to define an event. The number of values used in the averages for mass density is shown in the bottom panel (a) and (b).

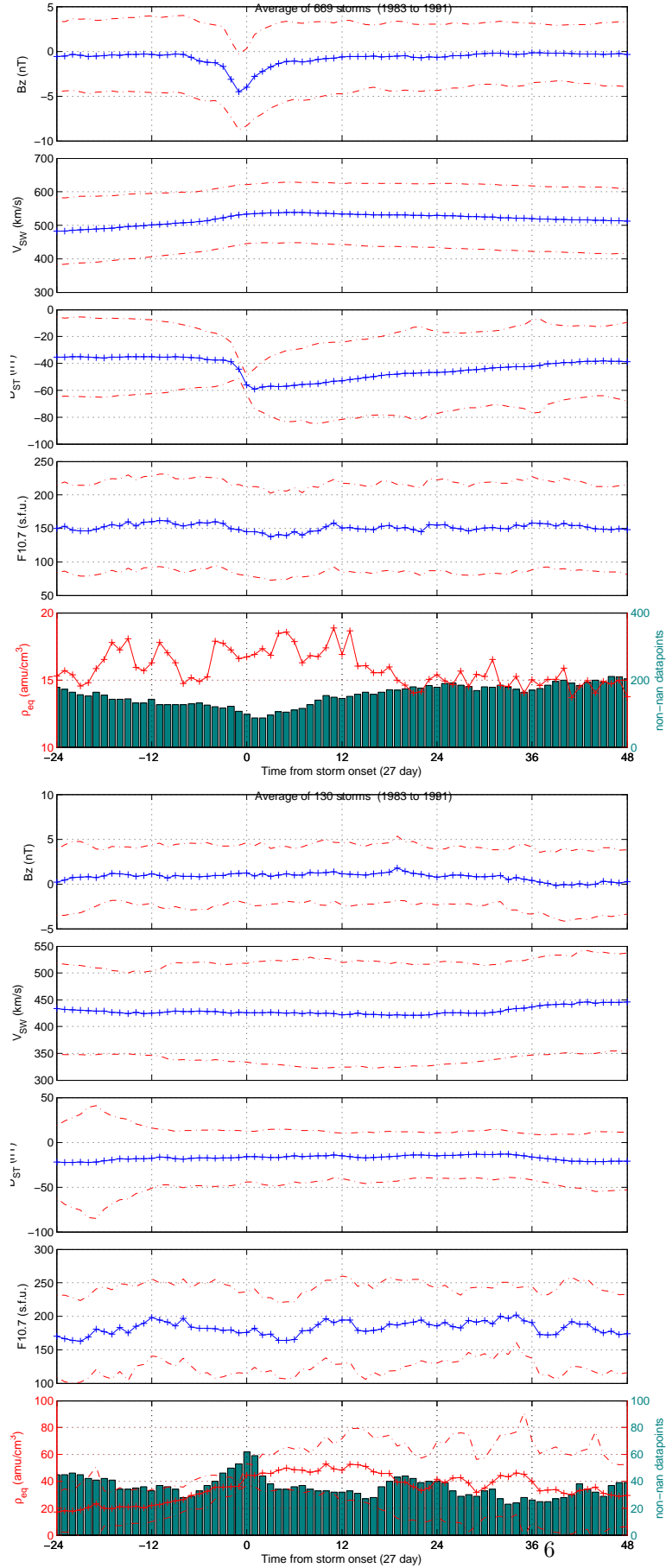


Figure 3: (a) Average of solar wind and near-Earth measurements around the time D_{st} crossed be-

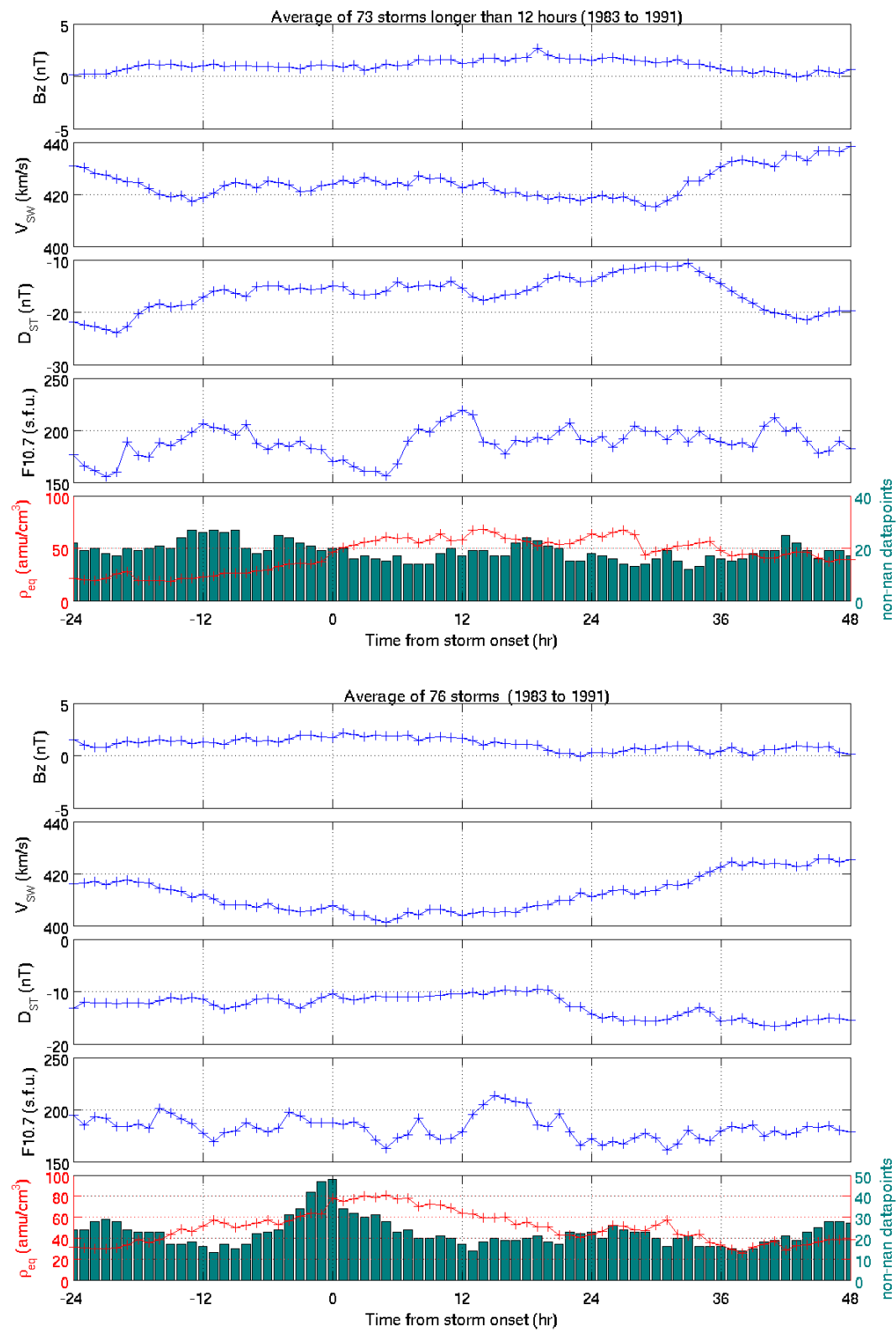
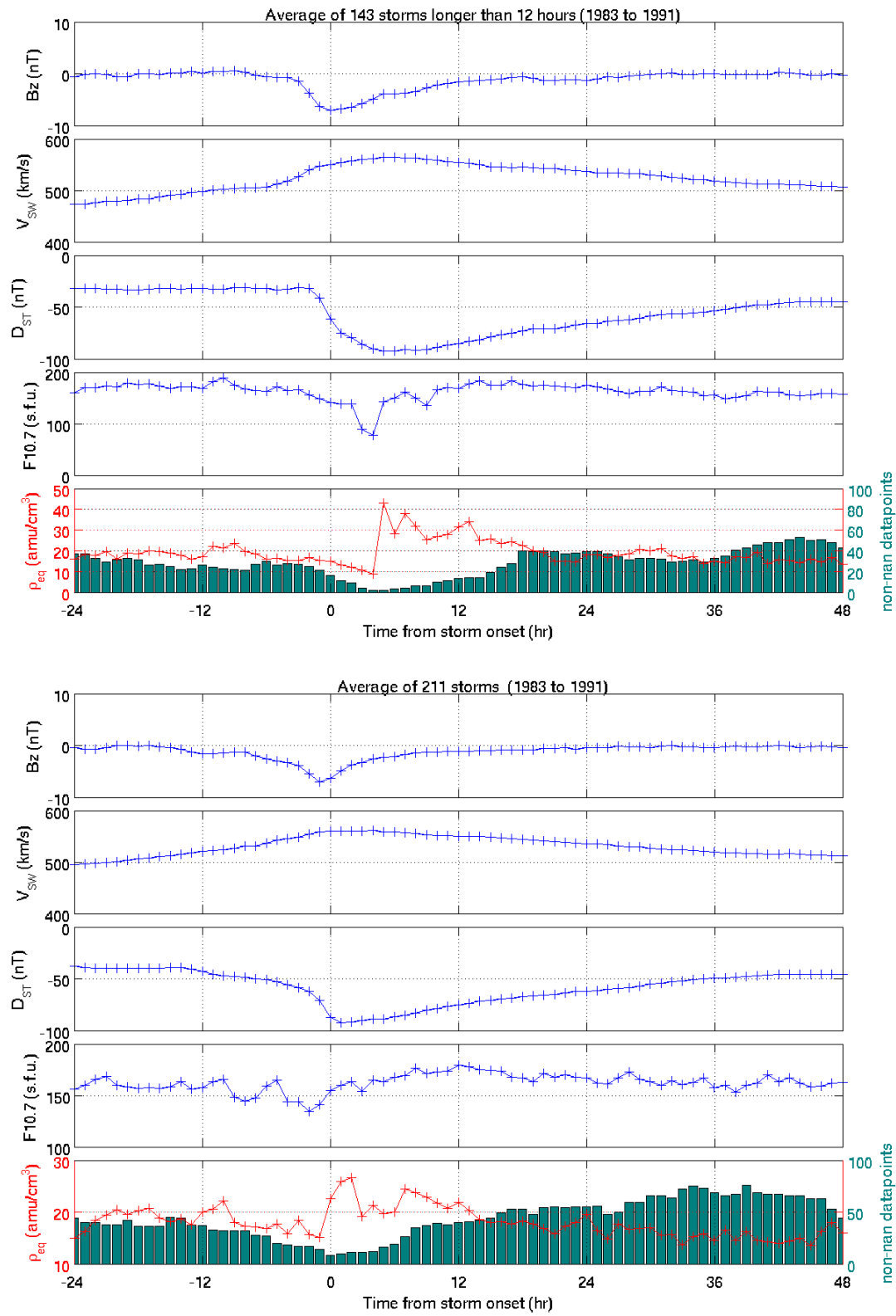


Figure 4: (a) Same as ??(a) except with constraint that D_{st} stayed below -40 nT for at least 12 hours. (b) Same as ??(b) except for constrain that mass density crossed above $70 \text{amu}/\text{cm}^3$.

Figure 5: D_{st} Storms > 12 hours, $D_{st} < -80nT$

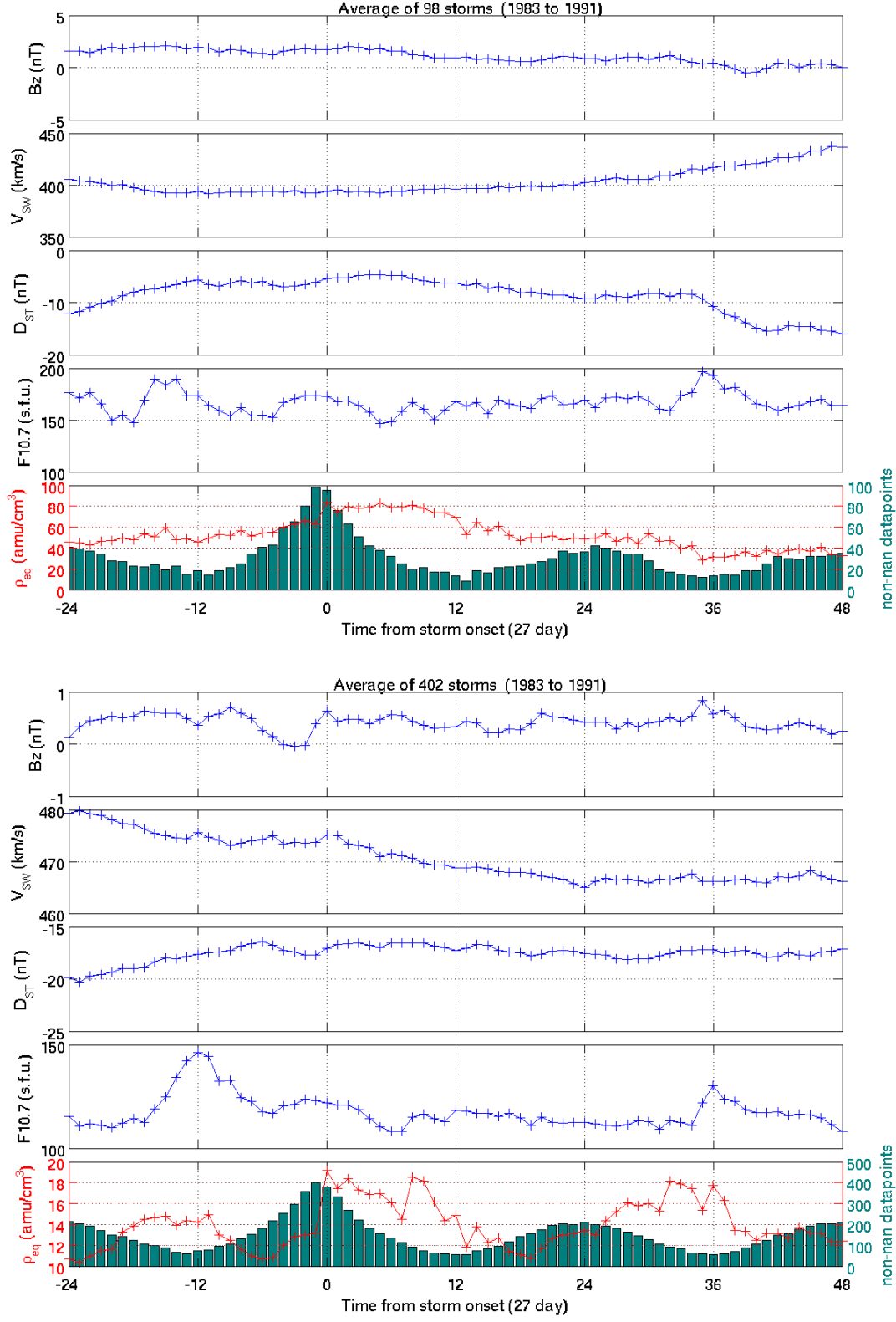


Figure 6: $\text{diff}(\rho_{eq}) > 20 \frac{\text{amu}}{\text{hour}}$, $\text{diff}(\rho_{eq}) > 30 \frac{\%}{\text{hour}}$

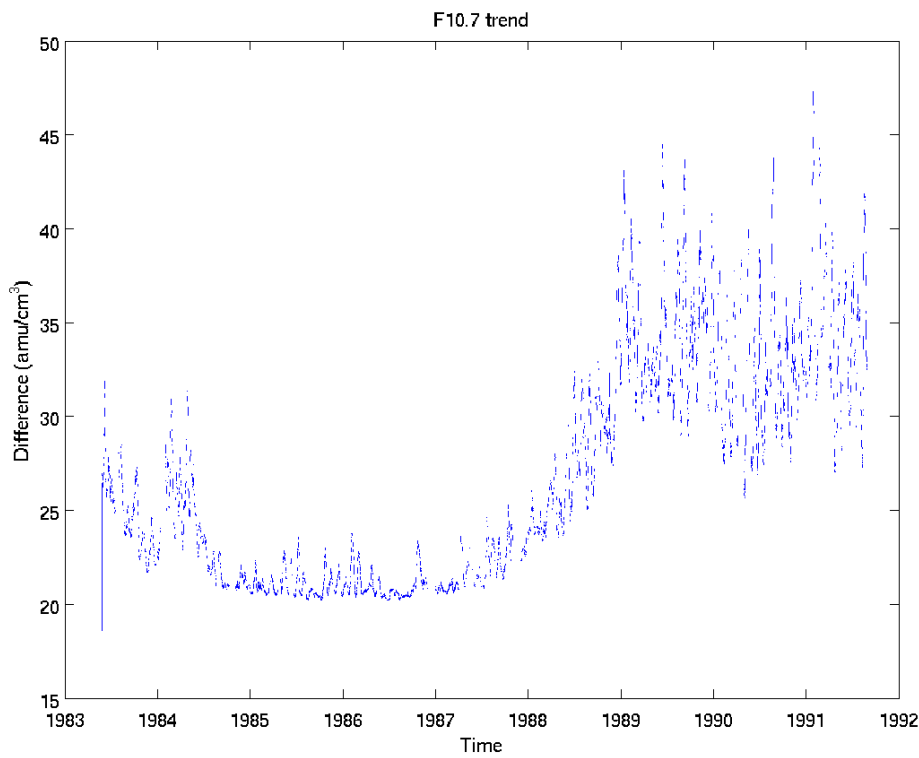
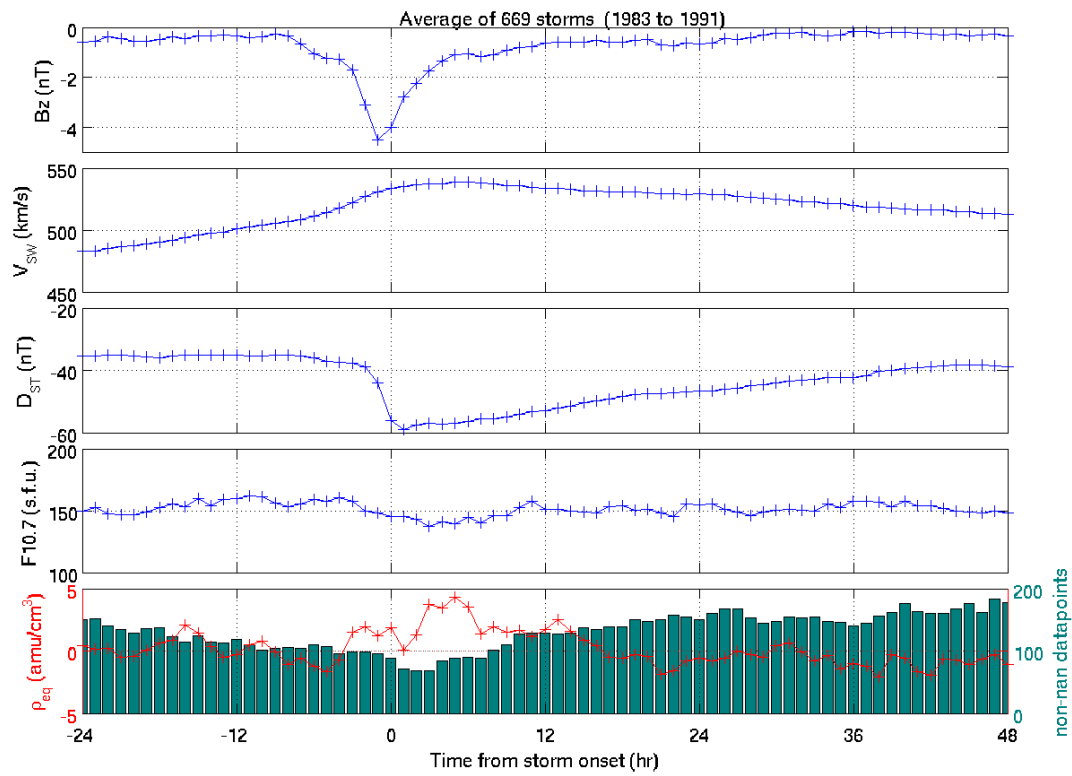


Figure 7: ρ_{eq} with $F_{10.7}$ removed, and Difference from original

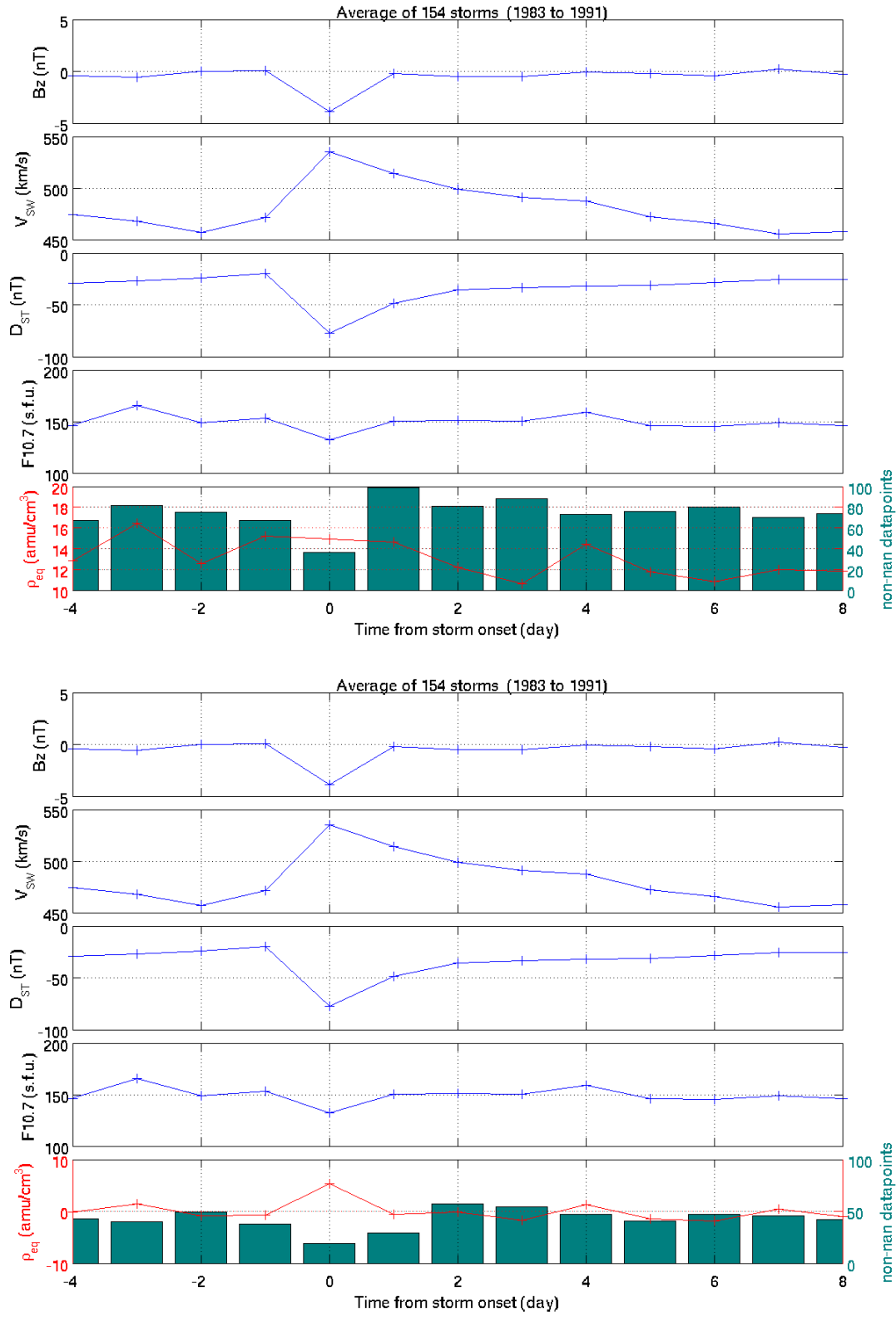


Figure 8: Original ρ_{eq} , and with $F_{10.7}$ dependence removed, both at 1-day averages